SUPPLEMENTAL FIGURES

Including: Figure S1 (relevant to Figure 1); Figure S2 (relevant to Figure 1); Figure S3 (relevant to Figure 3). Figure S4 (relevant to Figure 4). Figure S5 (relevant to Figure 6). Table S1 (relevant to Figures 1-6 and S1-S5). Table S3 (relevant to Figure 6). Table S4 (relevant to Key Resources Table).

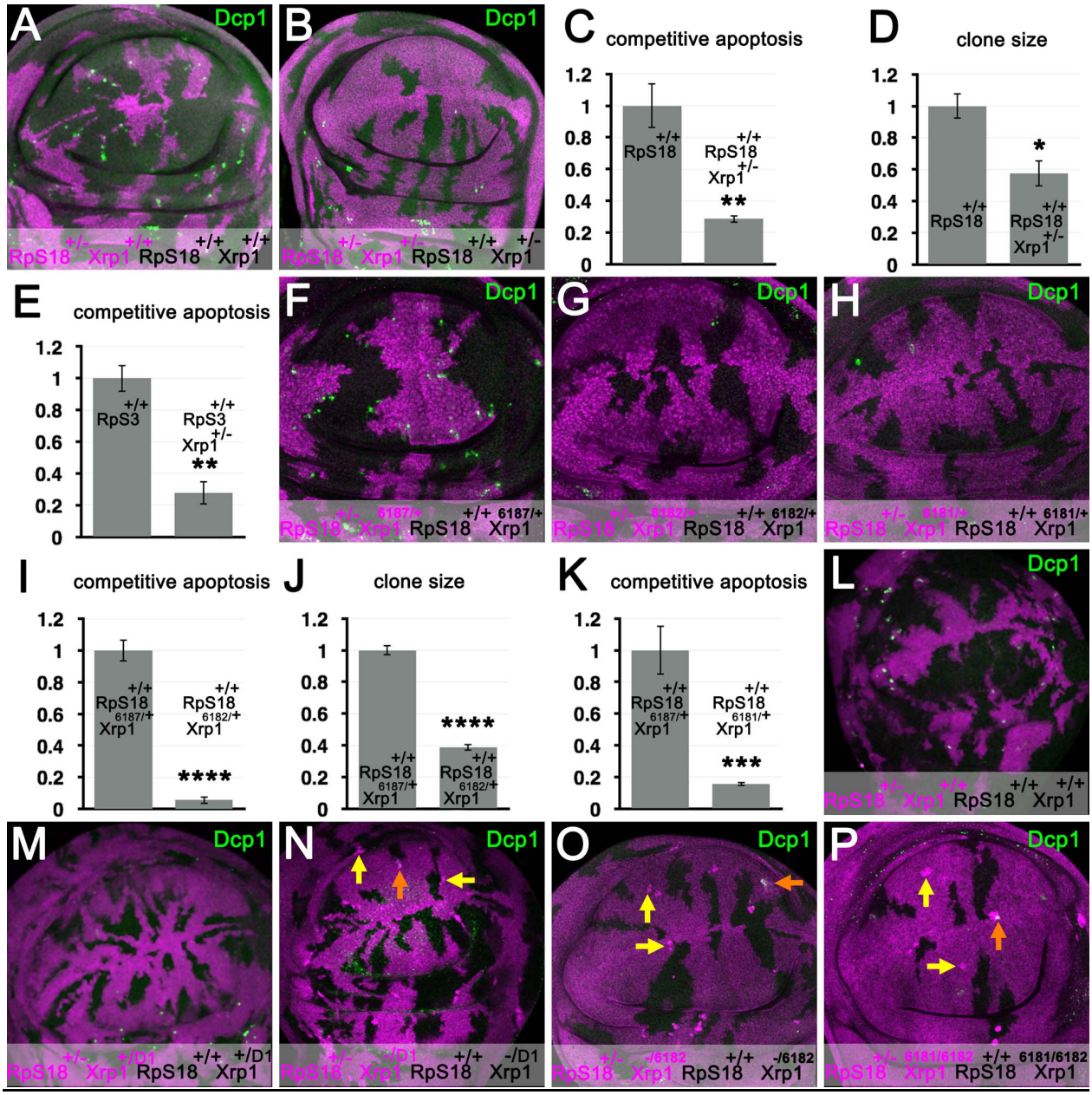

Figure S1. Related to Figure 1

A). Wing imaginal disc like that in Figure 1P, showing the growth and competition of wild type cells (unlabelled) in the *RpS18*$^{+/-}$ background (magenta). Dying cells labeled for active Dcp1 (green) are predominantly at the interfaces between wild type and *RpS18*$^{+/-}$ cells. B). Wing imaginal disc like that in Figure 1Q, showing the growth and competition of *Xrp1*$^{m2\text{-}73/+}$ cells (unlabelled) in the *RpS18*$^{+/-}$ *Xrp1*$^{m2\text{-}73/+}$ background (magenta). Competitive apoptosis is reduced and the *Xrp1*$^{m2\text{-}73/+}$ clones occupy less territory. C). Quantification of competitive apoptosis in *RpS18*$^{+/-}$ backgrounds. *RpS18*$^{+/+}$ *Xrp1*$^{m2\text{-}73/+}$ cells induced significantly less competitive apoptosis of *RpS18*$^{+/-}$ *Xrp1*$^{m2\text{-}73/+}$ cells than *RpS18*$^{+/+}$ *Xrp1*$^{+/+}$ cells induced in *RpS18*$^{+/-}$ *Xrp1*$^{m2\text{-}73/+}$. D). Quantification of growth in *RpS18*$^{+/-}$ backgrounds. *RpS18*$^{+/+}$ *Xrp1*$^{m2\text{-}73/+}$ cell clones grew to occupy significantly less of *RpS18*$^{+/-}$ *Xrp1*$^{m2\text{-}73/+}$ wing discs than *RpS18*$^{+/+}$ *Xrp1*$^{+/+}$ cells did in *RpS18*$^{+/-}$ *Xrp1*$^{m2\text{-}73/+}$ wing discs. E). Quantification of competitive apoptosis in *RpS3*$^{+/-}$ backgrounds as shown in Figures 1R-U. *RpS3*$^{+/+}$ *Xrp1*$^{m2\text{-}73/+}$ cells induced

significantly less competitive apoptosis of *RpS3*$^{+/-}$ *Xrp1*$^{m2\text{-}73/+}$ cells than *RpS3*$^{+/+}$ *Xrp1*$^{+/+}$ cells induced in *RpS3*$^{+/-}$ *Xrp1*$^{m2\text{-}73/+}$. F). Cell competition in wing imaginal disc heterozygous for *Df(3R)Exel6187*, a chromosomal deficiency that does not affect the *Xrp1* gene. Dying cells labeled for active Dcp1 (green) are predominantly at the interfaces between *RpS18*$^{+/+}$ *Df(3R)Exel6187*/+ cells and *RpS18*$^{+/-}$ *Df(3R)Exel6187*/+ cells. G). Mosaic wing imaginal disc heterozygous for *Df(3R)Exel6182*, a chromosomal deficiency that deletes part of the *Xrp1* gene (see map in Figure 1A). Competitive apoptosis is reduced and the *RpS18*$^{+/+}$ *Df(3R)Exel6182*/+ clones occupy less territory compared to *RpS18*$^{+/+}$ *Df(3R)Exel6187*/+ clones (compare panel F). H). Mosaic wing imaginal disc heterozygous for *Df(3R)Exel6181*, a chromosomal deficiency that deletes part of the *Xrp1* gene (see map in Figure 1A). Competitive apoptosis is reduced and the *RpS18*$^{+/+}$ *Df(3R)Exel6181*/+ clones occupy less territory compared to *RpS18*$^{+/+}$ *Df(3R)Exel6187*/+ clones (compare panel F). I). Quantitative comparison of competitive apoptosis in *Df(3R)Exel6187*/+ and *Df(3R)Exel6182*/+ backgrounds. Competitive apoptosis was significantly reduced by heterozygosity for *Df(3R)Exel6182*. J). Quantitative comparison of growth in *Df(3R)Exel6187*/+ and *Df(3R)Exel6182*/+ backgrounds. *RpS18*$^{+/+}$ *Df(3R)6182/+* cell clones grew to occupy significantly less of *RpS18*$^{+/-}$ *Df(3R)6182/+* wing discs than *RpS18*$^{+/+}$ *Df(3R)6187/+* cells did in *RpS18*$^{+/-}$ *Df(3R)6187/+* wing discs. K). Quantitative comparison of competitive apoptosis in *Df(3R)Exel6187*/+ and *Df(3R)Exel6181*/+ backgrounds. Competitive apoptosis was significantly reduced by heterozygosity for *Df(3R)Exel6181*. L). Positive control wing imaginal disc, showing the growth and competition of wild type cells (unlabelled) in the *RpS18*$^{+/-}$ background (magenta). Dying cells labeled for active Dcp1 (green) are predominantly at the interfaces between wild type and *RpS18*$^{+/-}$ cells. M). Mosaic wing imaginal disc heterozygous for *Xrp1*^{D1}, a mutation that deletes the *Xrp1* gene entirely (see map in Figure 1A). Competitive apoptosis is reduced and the *RpS18*$^{+/+}$ *Xrp1*$^{D1/+}$ clones occupy less territory in *RpS18*$^{+/-}$ *Xrp1*$^{D1/+}$ wing discs than *RpS18*$^{+/+}$ *Xrp1*$^{+/+}$ clones did in *RpS18*$^{+/-}$ *Xrp1*$^{+/+}$ wing discs (compare panel L). N). Mosaic wing imaginal disc homozygous for *Xrp1* mutations (*Xrp1*$^{m2\text{-}73/D1}$). Not only did *RpS18*$^{+/+}$ *Xrp1*$^{m2\text{-}73/D1}$ clones compete less with *RpS18*$^{+/-}$ *Xrp1*$^{m2\text{-}73/D1}$ cells than *RpS18*$^{+/+}$ *Xrp1*$^{+/+}$ clones did with *RpS18*$^{+/-}$ *Xrp1*$^{+/+}$ cells (compare panel L), but small clones of *RpS18*$^{-/-}$ *Xrp1*$^{m2\text{-}73/D1}$ clones survived 72h after induction (stronger labeling for ß-galactosidase, brighter magenta labeling; examples indicated by yellow arrows). Occasional *RpS18*$^{-/-}$ *Xrp1*$^{m2\text{-}73/D1}$ clones contained one or more apoptotic cells positive for active-Dcp1 (green; orange arrow). O). Mosaic wing imaginal disc homozygous for *Xrp1* mutations (*Xrp1*$^{m2\text{-}73}$/*Df(3R)Exel6182*). Not only did *RpS18*$^{+/+}$ *Xrp1*$^{m2\text{-}73}$/*Df(3R)Exel6182* clones compete less with *RpS18*$^{+/-}$ *Xrp1*$^{m2\text{-}73}$/*Df(3R)Exel6182* cells than *RpS18*$^{+/+}$ *Xrp1*$^{+/+}$ clones did with *RpS18*$^{+/-}$ *Xrp1*$^{+/+}$ cells (compare panel L), but small clones of *RpS18*$^{-/-}$ *Xrp1*$^{m2\text{-}73}$/*Df(3R)Exel6182* clones survived 72h after induction (stronger labeling for ß-galactosidase, brighter magenta labeling; examples indicated by yellow arrows). Occasional *RpS18*$^{-/-}$ *Xrp1*$^{m2\text{-}73}$/*Df(3R)Exel6182* clones contained one or more apoptotic cells positive for active-Dcp1 (green; orange arrow). P). Mosaic wing imaginal disc homozygous for *Xrp1* mutations (*Xrp1*$^{m2\text{-}73}$/*Df(3R)Exel6181*). Not only did *RpS18*$^{+/+}$ *Xrp1*$^{m2\text{-}73}$/*Df(3R)Exel6181* clones compete less with *RpS18*$^{+/-}$ *Xrp1*$^{m2\text{-}73}$/*Df(3R)Exel6181* cells than *RpS18*$^{+/+}$ *Xrp1*$^{+/+}$ clones did with *RpS18*$^{+/-}$ *Xrp1*$^{+/+}$ cells (compare panel L), but small clones of *RpS18*$^{-/-}$ *Xrp1*$^{m2\text{-}73}$/*Df(3R)Exel6181* clones survived 72h after induction (stronger labeling for ß-galactosidase, brighter magenta labeling; examples indicated by yellow arrows). Occasional *RpS18*$^{-/-}$ *Xrp1*$^{m2\text{-}73}$/*Df(3R)Exel6181* clones contained one or

more apoptotic cells positive for active-Dcp1 (green; orange arrow). Statistics: competitive apoptosis and wing disc territories occupied by genotypes were compared to the control genotype by t-test. Significance levels: $p<0.05$ (*); $p<0.01$ (**); $p<0.001$ (***); $p<0.0001$ (****). Data related to this Figure is shown in Table S1.

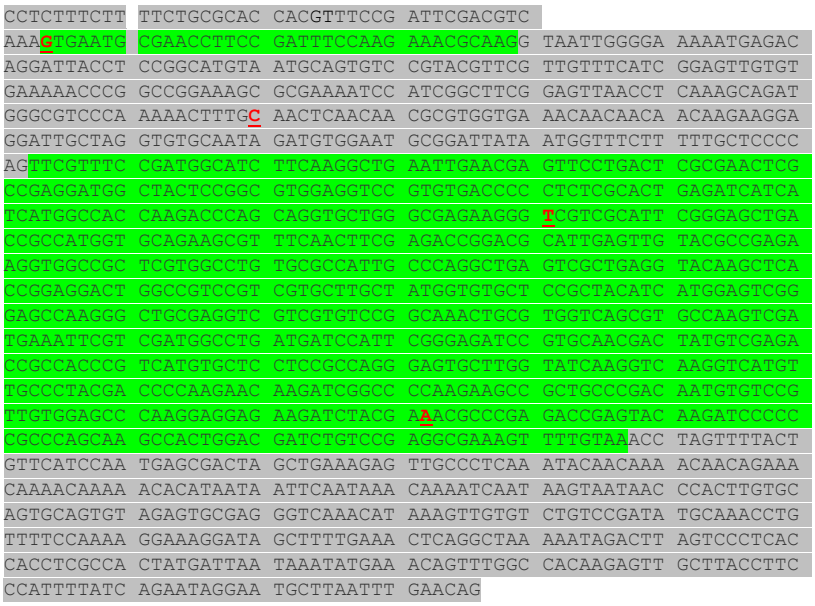

Figure S2 (relevant to Figure 1)
Genomic DNA sequence from the *RpS3* transcription unit. Open reading frame in green, interrupted by intron 1.. Sequence alterations from the reference sequences are indicated in red and underlined.

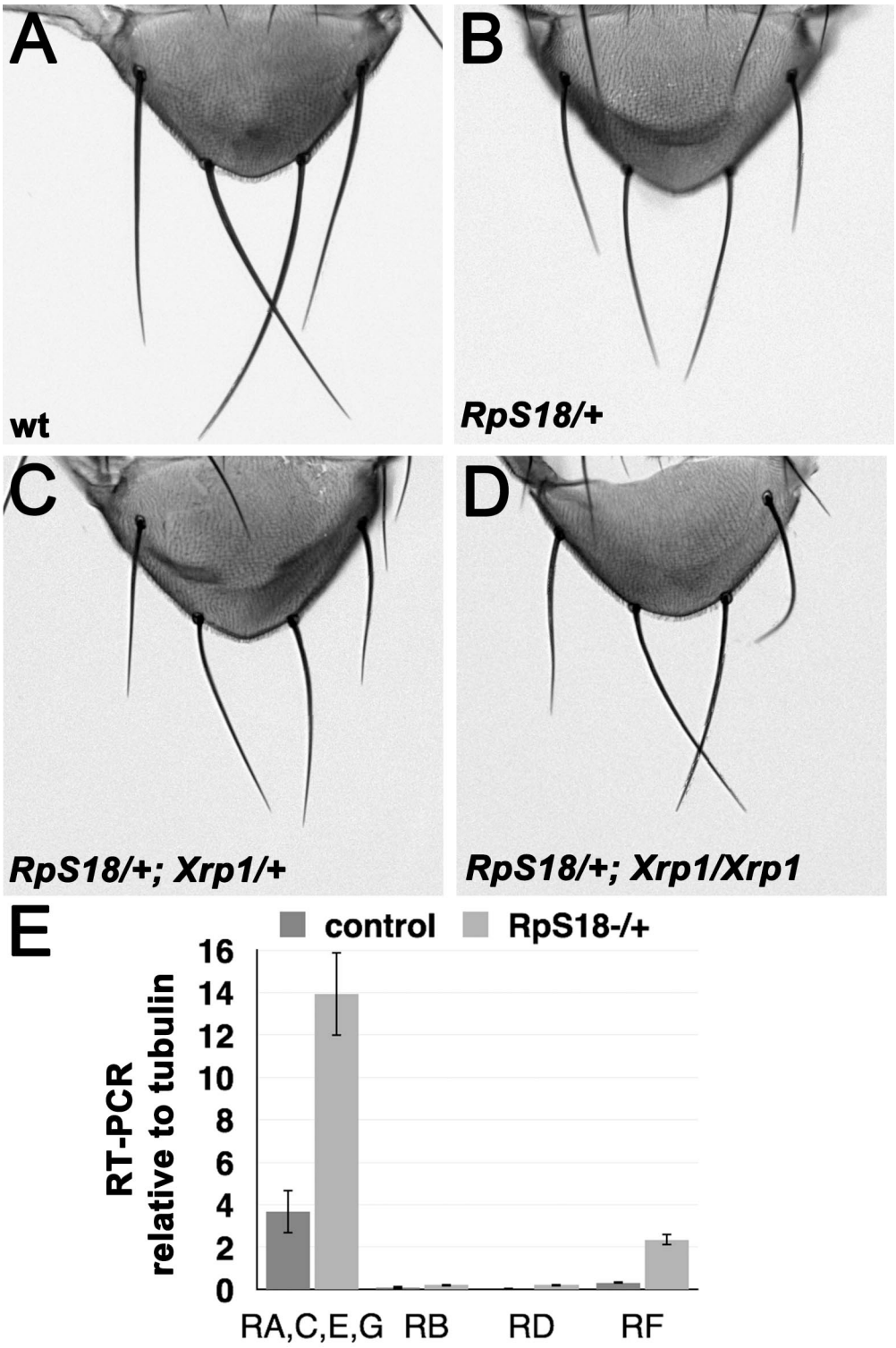

Figure S3. Related to Figure 3

A-D) Scutella from indicated genotypes. Images from main Figure 3A-B are repeated in panels A-B for comparison. E) mRNA levels presented relative to tubulin mRNA. The major *Xrp1* isoforms in wing imaginal discs include RA,C,E,G and RF, but RB and RD are expressed at low levels. Data related to this Figure is shown in Table S1.

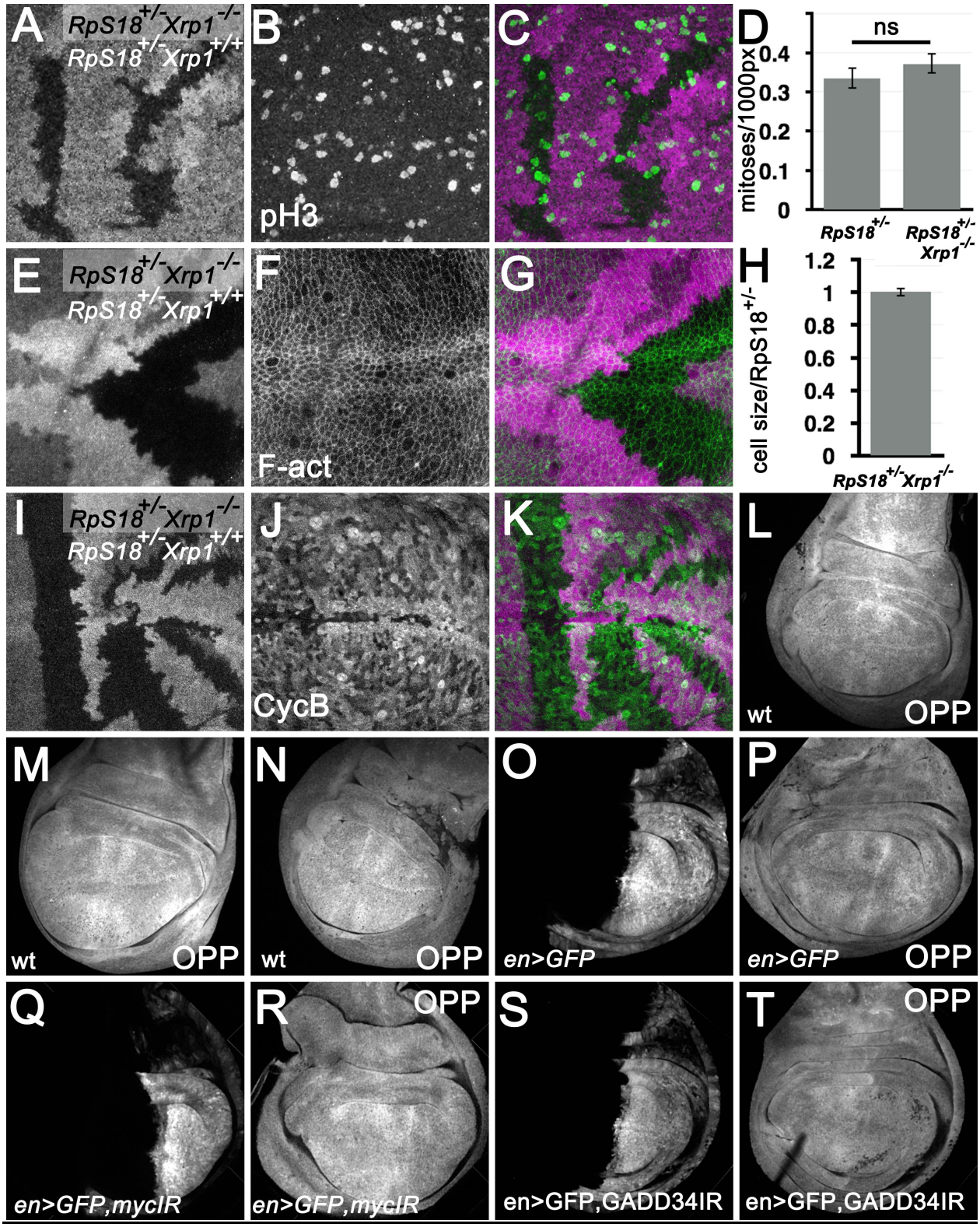

Figure S4. Related to Figure 4

A,E,I) Reciprocal clones of *Xrp1*$^{-/-}$ and *Xrp1*$^{+/+}$ cells (respectively unlabeled and brightly labeled by beta-galactosidase) in an *RpS18*$^{+/-}$ wing disc, similar to the experiment shown in Figure 3H. B) Mitotic cells labeled for phospho-Histone H3. C) Merge of panels A,B. D) Mitotic figures are slightly more frequent in *RpS18*$^{+/-}$ *Xrp1*$^{-/-}$ clones than *RpS18*$^{+/-}$ *Xrp1*$^{+/+}$ clones, but not significantly so (p=0.3583, paired t-test). Error bars

represent ±1 S.E.M. 612 mitotic cells were counted in 51 clones and 41 twins from 20 mosaic wing discs. F) Phalloiding labeling of F-actin labeling outlines cells in the wing disc shown in panel E). G) Merge of panels E,F. G) Cells in *RpS18*$^{+/-}$ *Xrp1*$^{-/-}$ clones do not differ significant in size from cells in *RpS18*$^{+/-}$ *Xrp1*$^{+/+}$ clones. (geometric mean ±1 S.E.M. of the log-transformed data). 4327 cells were measured in 17 clones and twin clones from 10 mosaic wing discs. J. Cyclin B protein identifies cells in S, G2, and early M-phase but is absent from G1-phase. K. Merge of panels I,J. No difference between G1-phase cells is apparent in the *RpS18*$^{+/-}$ *Xrp1*$^{-/-}$ and *RpS18*$^{+/-}$ *Xrp1*$^{+/+}$ genotypes. L,M,N) Further examples of OPP labeling of nascent proteins in wild type wing discs. O-P) GFP (O) and OPP (P) labeling of en-Gal4 UAS-GFP wing disc. GFP expression in the posterior compartment does not affect translation rate. Q-R) GFP Q) and OPP (R) labeling of en-Gal4 UAS-GFP UAS-*mycIR* wing disc. Note that *myc* knock down reduces posterior compartment size as well as translation rate. S-T). GFP (S) and OPP (T) labeling of en-Gal4 UAS-GFP UAS-*Gadd34IR* wing disc. Gadd34 knock down reduces translation rate in the posterior compartment. Data related to this Figure is shown in Table S1.

A

oxidation-reduction process

gene	AOX1	CG3902	CG10638	CG18547	Cyp6a14	Cyp6a20	Cyp6d2	Cyp6d4	Cyp6g2	Cyp6t3	Cyp9f2	ImpL3	Men	Nox	Sodh-2
RpS17/+	35.3	0.6	2.4	5.5	2.8	4.2	49.5	2.0	0.0	0.1	1.8	1.7	1.5	0.6	5.5
RpS3/+	47.4	0.7	2.3	5.6	2.2	5.0	21.5	1.5	0.0	0.0	1.6	2.6	1.7	0.7	4.5
RpS3/+ Xrp1/+	1.1	0.8	1.0	1.1	0.9	1.2	1.0	0.7	0.0	0.0	1.0	1.0	0.7	0.9	0.6

DNA repair, DSB repair, cellular response to γ-rays, DNA biosynthetic process

gene	CG5181	CG6171	Hus1-like	Ilp8
RpS17/+	1.7	1.6	2.0	22.1
RpS3/+	1.7	1.7	1.6	13.8
RpS3/+ Xrp1/+	2.0	1.0	1.1	1.1

immune response

gene	Dif	eater	Spz	Swim	Upd3
RpS17/+	3.5	2.7	3.2	1.9	3.0
RpS3/+	4.0	2.0	2.1	2.0	2.4
RpS3/+ Xrp1/+	0.9	2.3	1.7	1.3	0.7

B

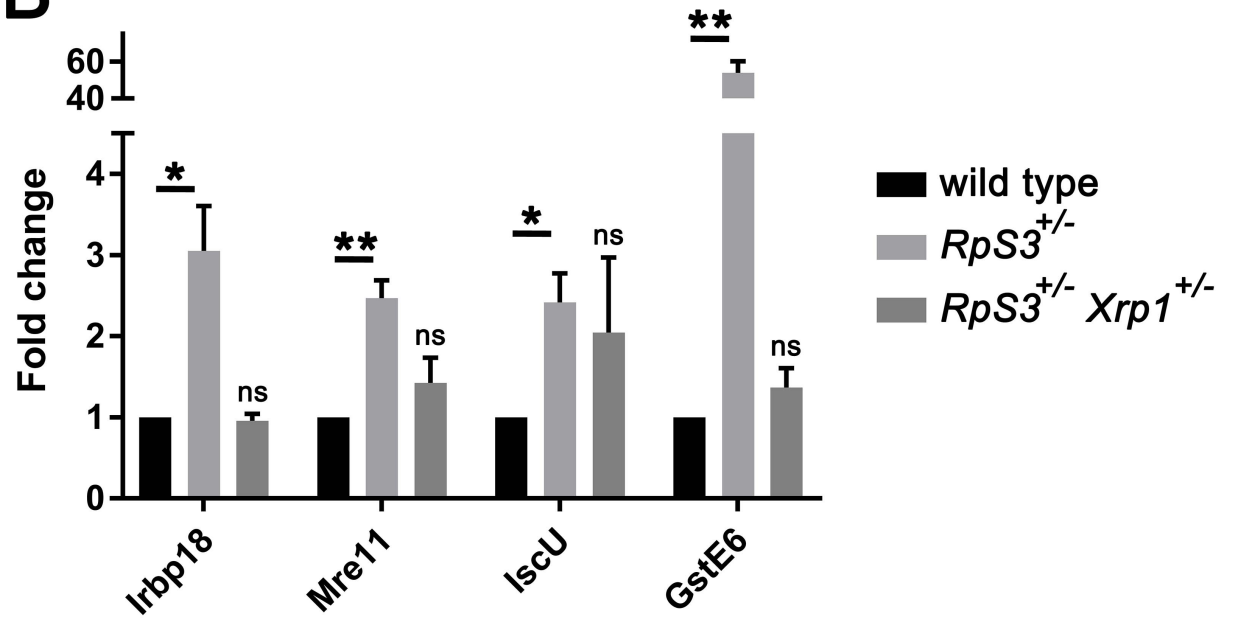

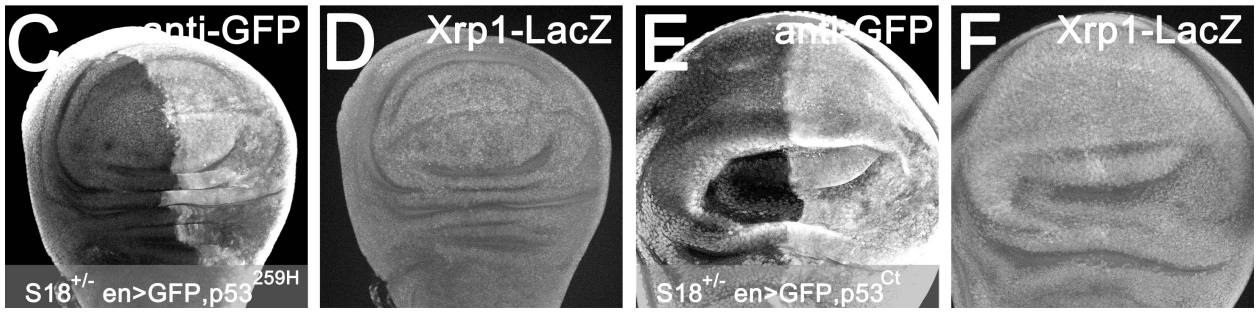

Figure S5. Related to Figure 6

A) Expression levels (fold changes relative to wild type control determined by Deseq2) are shown for Rp-regulated genes with the biological process GO term oxidation-reduction process, which is not statistically enriched among the 253 genes; additional Rp-regulated genes with the GO terms DNA repair, double-strand break repair, cellular response to gamma rays, cellular response to X-rays, DNA biosynthetic process, and with the GO terms immune response or stress-activated MAPK cascade (ie JnK signaling). Note also upregulation of *upd3*, a potential activator of the Jak-Stat pathway. None of these GO terms were statistically enriched among the 253 genes by our criteria. We also re-analyzed a set of 443 differentially-expressed genes identified by Kucinski et al (2017). We found these genes were enriched ($p<0.05$, Benjamini corrected) for the biological process GO terms oxidation-reduction process ($p=0.02$), glutathione metabolic process ($p=0.009$), and sensory perception of sweet taste

(p=0.012), but not for cellular stress response (no p value reported by DAVID). B) qRT-PCR validation of representative *Xrp1*-dependent, Rp-dependent transcripts. Fold change is shown in comparion to the wild type control. All the transcripts are more abundant in $RpS3^{+/-}$ wing discs (* represents $p<0.05$, ** represents $p<0.01$; two-tailed t-tests). None of the transcript levels differed between wild type and $RpS3^{+/-}$ $Xrp1^{+/-}$ wing discs (significantly (ie $p>0.05$). C) $RpS18^{+/-}$ wing imaginal disc in which UAS-GFP and UAS-$p53^{259H}$ were expressed in posterior cells under control of en-Gal4 and visualized with anti-GFP labeling. D) Expression of the *Xrp1* enhancer trap ($Xrp1^{02515}$) was unaffected by inhibiting p53 function. E) $RpS18^{+/-}$ wing imaginal disc in which UAS-GFP and UAS-$p53^{Ct}$ were expressed under control of en-Gal4. F) Expression of the *Xrp1* enhancer trap ($Xrp1^{02515}$) was unaffected by inhibiting p53 function. Data related to this Figure is shown in Tables S1-3.

SUPPLEMENTAL TABLES

Table S1.*Drosophila* Genotypes shown in Figures.
Relevant to Figures 1-6 and S1-S5.

Fig 1B, H,I : p{hs:FLP}; FRT82B p{arm:LacZ} RpS3/FRT82B
Fig 1C, J, K: p{hs:FLP}; FRT82B p{arm:LacZ} RpS3/FRT82B $Xrp1^{M2\text{-}73}$
Fig 1F: w Df(1)su(s)$R194^{-}$/p{ey:FLP}; FRT82B p{$RpL36^{+}$} p{arm:LacZ} /FRT82
Fig 1G: w Df(1)su(s)$R194^{-}$/p{ey:FLP}; FRT82B p{$RpL36^{+}$} p{arm:LacZ} /FRT82 $Xrp1^{M2\text{-}73}$
Fig 1L-M, P: p{hs:FLP}; FRT42 RpS18 p{ubi:GFP} /FRT42
Fig 1N-O, Q: p{hs:FLP}; FRT42 RpS18 p{ubi:GFP} /FRT42; FRT82B $Xrp1^{M2\text{-}73}$/+
Fig 1R: p{hs:FLP}; FRT82B RpS3/FRT82B p{arm:LacZ}
Fig 1S: p{hs:FLP}; FRT82B RpS3 $Xrp1^{M2\text{-}73}$ /FRT82B p{arm:LacZ}
Fig 1T,U: p{hs:FLP}; FRT82B $Xrp1^{M2\text{-}73}$ RpS3 /FRT82B p{arm:LacZ}

Fig2A,C: $w^{11\text{-}18}$
Fig2B,D:Df(3R)Exel6181/Df(3R)Exel6182

Fig 3A: p{hs:FLP}; FRT82B p{arm:LacZ}/FRT82B $Xrp1^{M2\text{-}73}$
Fig 3B: p{hs:FLP}; FRT42 $RpS18^{-}$ p{ubi:GFP} /+;FRT82B p{arm:LacZ}/FRT82B $Xrp1^{M2\text{-}73}$
Fig 3D: FRT82B p{arm:LacZ} RpS3/FRT82
FRT82B p{arm:LacZ} RpS3/FRT82 $Xrp1^{M2\text{-}73}$
FRT82 $Xrp1^{M2\text{-}73}$/TM6B
FRT82/TM6B
Fig 3E: FRT42D RpS18 p{ubi:GFP}/+; FRT82B/+
FRT42D RpS18 p{ubi:GFP}/+; FRT82B $Xrp1^{M2\text{-}73}$/+
FRT42D RpS18 p{ubi:GFP}/+; FRT82B $Xrp1^{M2\text{-}73}$/Df(3R)Exel6181
FRT42D
Fig 3F: $w^{11\text{-}18}$/FM7
$w^{11\text{-}18}$/FM7; Df(3R)Exel6182/+
$w^{11\text{-}18}$/w Df(1)su(s)R194
$w^{11\text{-}18}$/w Df(1)su(s)R194; Df(3R)Exel6182/+
Fig 3G: $w^{11\text{-}18}$
Fig 3H: FRT82B p{arm:LacZ} RpS3/$w^{11\text{-}18}$
Fig 3J: FRT42D RpS18 p{ubi:GFP}/CyO
Fig3K-L: p{hs:FLP}; FRT42 $RpS18^{-}$ p{ubi:GFP} /FRT42; FRT82B $Xrp1^{02515}$/+
Fig3K-L: p{hs:FLP}; FRT42 $RpS18^{-}$ p{ubi:GFP} /FRT42
Fig 3M,N: FRT42 $RpS18^{-}$ p{ubi:GFP}/FRT42
Fig3O: GMR-Gal4/+
Fig 3P: GMR-Gal4/+; UAS-Xrp1(Flag-CDS2)

Fig4A-B, E: yw; p{arm:LacZ} FRT80B
Fig4C-D: p{hs:FLP}; p{ubi:GFP} FRT40 /Tor^{DP} FRT40
Fig4F-J: p{hs:FLP}; FRT42 $RpS18^{-}$ p{ubi:GFP} /FRT42
Fig4K-L, O-P: p{hs:FLP}; M(3)67c p{ubi:GFP} FRT80B/FRT80B
Fig4M-N: p{hs:FLP}; $RpL27A^{-}$ p{arm:LacZ} FRT40/FRT40

Fig4Q-T: p{hs:FLP}; FRT42 RpS18^{-} p{ubi:GFP} /FRT42; FRT82B Xrp1$^{M2\text{-}73}$/+

Fig 5:
Wild type genotype: p{hs:FLP}/w^{118}; p{arm:LacZ} FRT80B/+
Xrp1/+ genotype: p{hs:FLP}/w^{118}; FRT82B Xrp1$^{M2\text{-}73}$/+
RpL27A/+ genotype: p{hs:FLP}/ p{hs:FLP}; RpL27A^{-} p{arm:LacZ} FRT40/+; FRT80B/+
RpL27A/+; Xrp/+ genotype: p{hs:FLP}/ p{hs:FLP}; RpL27A^{-} p{arm:LacZ} FRT40/+; FRT82B Xrp1$^{M2\text{-}73}$/+
RpS18/+ genotype: p{hs:FLP}/ p{hs:FLP}; FRT42 RpS18 p{ubi:GFP} /+; FRT80B/+
RpS18/+; Xrp/+ genotype: p{hs:FLP}/ p{hs:FLP}; FRT42 RpS18 p{ubi:GFP} /+; FRT82B Xrp1$^{M2\text{-}73}$/+
RpS3/+ genotype: p{hs:FLP}/ p{hs:FLP}; FRT42/+; FRT82 RpS3 p{arm:LacZ} /+
RpS3/+; Xrp/+ genotype: p{hs:FLP}/ p{hs:FLP}; FRT82 RpS3 p{arm:LacZ} /FRT82B Xrp1$^{M2\text{-}73}$

Fig6A-E: w$^{1\text{-}18}$/+; FRT82B/+
w$^{1\text{-}18}$/y w p{hs:FLP}; FRT82 RpS3 p{arm:LacZ/+
w$^{1\text{-}18}$/y w p{hs:FLP}; RpS17 p{ubi:GFP} FRT80B/+
w$^{1\text{-}18}$/y w p{hs:FLP}; FRT82 RpS3 p{arm:LacZ/FRT82B FRT82B Xrp1$^{M2\text{-}73}$
Fig6F,G: p{hs:FLP}/ p{hs:FLP}; M(3)67c p{ubi:GFP} FRT80B/FRT80B
Fig6H,I: p{hs:FLP}/ p{hs:FLP}; M(3)67c p{ubi:GFP} RpS12^{G97D} FRT80B/ RpS12^{G97D} FRT80B
Fig 6J,K: p{hs:FLP}; FRT42 RpS18^{-}/UAS-RpS12-Flag;act>STOP>Gal4, UAS-His-RFP/+
Fig 6L,M: p{hs:FLP}; FRT42 RpS18^{-} p{ubi:GFP} /FRT42; FRT82B Xrp^{02515}/+
Fig 6N,O: p{hs:FLP}; FRT42 RpS18^{-} p{ubi:GFP} /FRT42; RpS12^{G97D} FRT80B Xrp^{02515}/ RpS12^{G97D} FRT80B

FigS1A: p{hs:FLP}; FRT42 RpS18 p{arm:lacZ} /FRT42
Fig S1B: p{hs:FLP}; FRT42 RpS18 p{arm:lacZ} /FRT42; FRT82B Xrp1$^{M2\text{-}73}$/+
FigS1F: p{hs:FLP}; FRT42 RpS18 p{arm:lacZ} /FRT42; Df(3R)Exel6187/+
Fig S1G: p{hs:FLP}; FRT42 RpS18 p{arm:lacZ} /FRT42; Df(3R)Exel6182/+
Fig S1H: p{hs:FLP}; FRT42 RpS18 p{arm:lacZ} /FRT42; Df(3R)Exel6181/+
FigS1L: p{hs:FLP}; FRT42 RpS18 p{arm:lacZ} /FRT42
Fig S1M: p{hs:FLP}; FRT42 RpS18 p{arm:lacZ} /FRT42; Xrp1^{D1}/+
Fig S1N: p{hs:FLP}; FRT42 RpS18 p{arm:lacZ} /FRT42; Xrp1^{D1}/ FRT82B Xrp1$^{M2\text{-}73}$
Fig S1O: p{hs:FLP}; FRT42 RpS18 p{arm:lacZ} /FRT42; Df(3R)Exel6182/ FRT82B Xrp1$^{M2\text{-}73}$
Fig S1P: p{hs:FLP}; FRT42 RpS18 p{arm:lacZ} /FRT42; Df(3R)Exel6181/ Df(3R)Exel6182

Fig S2A: FRT82B RpS3 p{arm-LacZ}/FRT82B and FRT82B

Fig S3A: FRT42D
Fig S3B; FRT42D RpS18 p{ubi:GFP}/+; FRT82B/+
FIG S3C: FRT42D RpS18 p{ubi:GFP}/+; FRT82B Xrp1$^{M2\text{-}73}$/+
FIG S#D: FRT42D RpS18 p{ubi:GFP}/+; FRT82B Xrp1$^{M2\text{-}73}$/Df(3R)Exel6181

FigS4A-K: p{hs:FLP}; FRT42 RpS18 p{ubi:GFP} /+; FRT82B p{arm:lacZ} / FRT82B $Xrp1^{M2\text{-}73}$
FigS4L-N: yw; p{arm:LacZ} FRT80B
FigS4O,P: yw; en-GAL4, UAS-GFP
FigS4Q,R: yw; en-GAL4, UAS-GFP;UAS-mycRNAi
FigS4S,T: yw; en-GAL4, UAS-GFP;UAS-Gadd34RNAi

Fig S5B:
$w^{1\text{-}18}$/+; FRT82B/+
$w^{1\text{-}18}$/y w p{hs:FLP}; FRT82 RpS3 p{arm:LacZ/+
$w^{1\text{-}18}$/y w p{hs:FLP}; RpS17 p{ubi:GFP} FRT80B/+
$w^{1\text{-}18}$/y w p{hs:FLP}; FRT82 RpS3 p{arm:LacZ/FRT82B FRT82B $Xrp1^{M2\text{-}73}$
Fig S5C,D: p{hs:FLP}/+; FRT42 RpS18/p{en-Gal4} p{UAS-GFP}; p{UAS-p53.259H}/Xrp^{02515}
Fig S5E,F: p{hs:FLP}/+; FRT42 RpS18/p{en-Gal4} p{UAS-GFP}; p{UAS-p53.Ct}/Xrp^{02515}

Table S3. 159 Genes significantly altered in $Rp^{+/-}$ genotypes both this study and in Kucinski et al (2017). Related to Figure 6.

Supplemental Table 3. Genes differentially regulated in *RpS3*/+ and *RpS17*/+ (this study) and in *RpS3*/+ and *RpS3**/+ (Kucinski et al 2017).

AOX1	Ady43A	Arc1	Arc2	Archease	Bin1
Brd	CG10005	CG10189	CG10445	CG10559	CG10638
CG10916	CG11710	CG11897	CG12099	CG12224	CG12264
CG12868	CG13258	CG14304	CG14314	CG14695	CG14906
CG14907	CG15784	CG1582	CG16787	CG17327	CG17574
CG17904	CG18213	CG18547	CG18596	CG1882	CG2064
CG2076	CG2909	CG3008	CG30196	CG3036	CG31140
CG31549	CG31875	CG31918	CG31955	CG32549	CG32625
CG32641	CG32694	CG33158	CG33509	CG3448	CG3788
CG42362	CG42363	CG42365	CG42598	CG43326	CG43366
CG44194	CG4858	CG5535	CG5664	CG6171	CG6330
CG6512	CG7080	CG7201	CG7367	CG7627	CG8192
CG8303	CG8549	CG9411	CHKov2	CIAPIN1	CRMP
Cda5	Cul2	Cyp6a20	Cyp6d2	Cyp6d4	Cyp6g2
Cyp6t3	Cyp9f2	Dif	Dscam3	Ets21C	Exn
Gadd45	Gclc	Gcn5	Gr64b	Gr64d	GstE1
GstE3	GstE5	GstE6	GstE7	GstE8	GstT1
HBS1	Ilp8	ImpL3	Ir40a	Irbp	Irbp18
IscU	Jheh1	Ku80	Lig4	MRP	Men
Mocs1	NKCC	Nep2	Obp99a	Osi14	Qtzl
Rack1	RpA-70	RpS27A	RpS9	Snap25	SoYb
Sodh-2	Spn47C	Swim	Traf4	Tsp42Ed	Ttc19
Ugt86Da	Ugt86Di	Xrp1	agt	amd	baz
dpr6	drd	eIF6	eater	lama	lig3
mre11	mus205	na	nsr	obe	pgant8
ppk13	ppk29	rad50	rpk	sra	unc-13
upd3	ver	wus			

Table S4. Oligonucleotides used in this study.

Table S4. Oligonucleotides used in the study. Relevant to Key Resources Table		
For 18S probe: GGTGCTGAAGCTTATGTAGC	Invitrogen	
For 18S probe: TAATACGACTCACTATAGGGAGACAAAGGGCAGGGACG	Invitrogen	
For 5.8S probe: GCTTATATGAAACTAAGACATTTCG	Invitrogen	
For 5.8S probe: TAATACGACTCACTATAGGGTACATAACAGCATGGACTGC	Invitrogen	
For tubulin probe: GCCCGTGGCCACTACACCATCGG	Invitrogen	
For tubulin probe: TAATACGACTCACTATAGGGAAGTGAATACGTGGGTAGGG	Invitrogen	
For actin probe: CCCCATTGAGCACGGTATCG	Invitrogen	
For actin probe: TAATACGACTCACTATAGGGAGAAAGAGTAACCGCGCTCG	Invitrogen	
Primer, Xrp1-RA, RC, RE, RG forward: TCATCGCGGAACAATAACAGTG	This paper	N/A
Primer, Xrp1-RA, RC, RE, RG reverse: GCAATAGGTTGGGTGGTTCC	This paper	N/A
Primer, Xrp1-RB forward: ACCGGAGATAAGGAGCAACA	This paper	N/A
Primer, Xrp1-RB forward: ACCGGAGATAAGGAGCAACA	This paper	N/A
Primer, Xrp1-RD forward: TAAGAGGTGTTTTTGGTCCGC	This paper	N/A
Primer, Xrp1-RD reverse: TCCTTTCCGTTTTCGCTGTTG	This paper	N/A
Primer, Xrp1-RF forward: CAACCACGTAACCACCCATCT	This paper	N/A
Primer, Xrp1-RF reverse: GGGATCTCGAGGATACGCCTG	This paper	N/A
Primer, α-Tubulin forward: TGTGAATTTTCCTTGTCGCGT	This paper	N/A
Primer, α-Tubulin reverse: CCAGCAGGCGTTTCCAATC	This paper	N/A
Primer, Irbp18 forward: TTCGCCATTAAGTCCGCACA	This paper	N/A
Primer, Irbp18 reverse: GTTCCTCGGCCGATTTCTTG	This paper	N/A
Primer, Mre11 forward: GGGCCAGCTAGATGTGACAG	This paper	N/A
Primer, Mre11 reverse: GGCAGTATTACGAGAGCCCA	This paper	N/A
Primer, IscU forward: TGGCATTAGGTCGTAGTATGCG	This paper	N/A
Primer, IcsU reverse: GCACTTATCAGCAGTCACGC	This paper	N/A
Primer, GstE6 forward: AAAGATCCTCTCAAGCGGGC	This paper	N/A
Primer, GstE6 reverse: CTGTCCCTGGAAGAGCACTG	This paper	N/A
Primer, CG13220 forward: AGCCCTTGCGGTGAATGTTA	This paper	N/A
Primer, CG13220 reverse: ACACGTTCGTCAGGTCCTTC	This paper	N/A